www.czasopisma.pan.pl PAN POLSKA AKADEMIA NAUK www.journals.pan.pl

Arch. Metall. Mater. **70** (2025), 4, 1499-1505

DOI: https://doi.org/10.24425/amm.2025.156230

ZHAO JIANG[1*], ZHANJI MA[1], SHUILIAN LUO[1], YANSHUAI ZHANG[1]

# RESEARCH ON UNIFORM GAS DISTRIBUTION IN CATHODE SYSTEM OF PVD COATING EQUIPMENT FOR CUTTING TOOLS

To resolve coating appearance non-uniformity in industrial PVD-coated cutting tools, this study investigates cathode system gas distribution optimization. By analyzing the gas flow characteristics of single-nozzle-type gas pipelines, finite element simulations were employed to compare gas flow fields under equal hole spacing and gradient hole spacing configurations. Structural optimizations, including downward nozzle orientation and diffusion space enlargement, were proposed to eliminate jet flow effects. Experimental results demonstrated that the gradient hole spacing design significantly improved coating uniformity. Energy-dispersive spectroscopy (EDS) analysis revealed that the carbon content deviation among upper, middle, and lower samples was less than 10%, effectively resolving axial chromatic inconsistencies. This work establishes theoretical frameworks and technical protocols for PVD gas distribution uniformity, advancing product quality and batch consistency.

*Keywords:* PVD coating; Cathode system; Uniform gas distribution; Finite element simulation; Coating appearance uniformity

## 1. Introduction

In industrial-scale PVD (Physical Vapor Deposition) tool coating production, while physical properties such as coating thickness, hardness, adhesion strength, and wear resistance remain critical quality indicators [1-3], the visual consistency of coated tools has emerged as an equally vital parameter. This characteristic not only impacts product aesthetics and quality perception, but also serves as a key technical metric for evaluating PVD coating equipment performance [4]. Coating non-uniformity primarily manifests as thickness variation and compositional heterogeneity, both being complex engineering challenges influenced by multiple interdependent process parameters during PVD deposition [5].

Current industry practices predominantly focus on optimizing deposition temperature, cathode magnetic field configuration, and discharge parameters to mitigate chromatic aberrations [4-6]. However, such adjustments exhibit limited effectiveness and may inadvertently compromise essential mechanical properties. Particularly for multi-component compound coatings like TiCN (commonly applied to tap surfaces), stoichiometric ratio variations constitute the most direct cause of color inconsistency [7-9]. The critical yet frequently overlooked factor in compositional uniformity control lies in the gas distribution dynamics within the cathode system [10]. Existing research predominantly focuses on theoretical analyses with limited practical applicability. To achieve visually uniform, high-quality coatings, rational gas distribution system design represents a crucial technological approach.

This study presents a systematic investigation into gas flow optimization through finite element simulation coupled with experimental validation. By analyzing the spatial configuration of cathode targets and implementing computational fluid dynamics modeling, we propose an optimized gas distribution structure design. The developed methodology demonstrates significant potential for enhancing coating uniformity while maintaining superior mechanical performance, thereby providing valuable insights for quality improvement in industrial PVD coating applications.

## 2. Gas Distribution Structure Mechanism Analysis

The gas distribution structure serves as the fundamental determinant of working gas dispersion within the deposition chamber, directly governing the spatial uniformity of gas flow. Fig. 1 illustrates the schematic configuration of a planar cathode system's gas distribution mechanism. As shown, gas distribution pipes are symmetrically positioned along both sides of the planar

[1] NATIONAL KEY LABORATORY ON VACUUM TECHNOLOGY AND PHYSICS, LANZHOU INSTITUTE OF PHYSICS, LANZHOU 730000, P.R. CHINA

* Corresponding author email: qqq-128@163.com

cathode target. The working gas undergoes collision, diffusion, and redistribution processes after exiting the pipes, ultimately achieving uniform longitudinal dispersion along the cathode target surface. This uniformity is essential for maintaining consistent plasma distribution, which ensures homogeneous target erosion and stable ionization reactions across the cathode's entire working length [11,12].

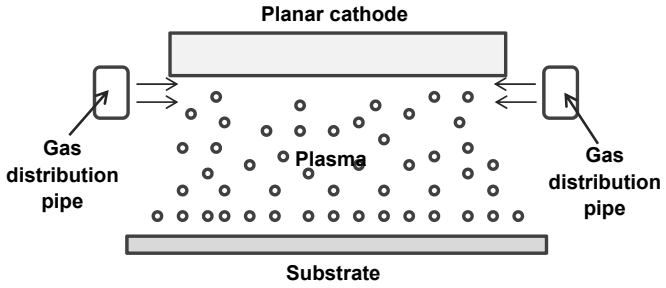


Fig. 1. Schematic of gas distribution structure in a planar cathode system

Figs. 2a and 2b present two prevalent industrial gas distribution configurations: the nozzle-type single-pipe system and the binary-type multi-pipe system [13]. The nozzle-type configuration (Fig. 2a) utilizes a single-layer pipe with equidistant micro-orifices, enabling gas flow from inlet to nozzle-shaped outlets. In contrast, the binary-type system (Fig. 2b) utilizes multi-stage uniformly symmetric piping networks. Gas sequentially traverses primary and secondary conduits before exiting through terminal outlets.

Notably, while the binary-type configuration theoretically enhances symmetry, its practical implementation faces significant challenges. Subsidiary pipelines demand strict geometric symmetry, necessitating exceptional machining precision and assembly tolerances. Furthermore, thermal expansion and operational deformation during prolonged use inevitably disrupt this symmetry, leading to gas flow inconsistencies. Consequently, industrial planar cathode systems predominantly adopt the mechanically robust nozzle-type configuration, despite its inherent limitations in gas distribution refinement.

Figs. 2a and 2b illustrate the schematic diagrams of two predominant gas distribution configurations employed in industrial applications: the nozzle-type single-pipe system and the binary-type multi-pipe system. The nozzle-type configuration (Fig. 2a) consists of a single-layer distribution pipe with uniformly spaced micro-orifices, where the working gas enters through the inlet and exits via nozzle-like apertures. In contrast, the binary-type system (Fig. 2b) comprises a multi-stage network of symmetrically interconnected pipes. The working gas sequentially flows from the primary conduit into subsequent secondary pipelines before exiting through multiple outlets. However, the binary-type configuration faces significant practical limitations. Its strict requirement for geometric symmetry across all subsidiary pipelines imposes stringent demands on machining precision and assembly tolerances. Moreover, thermal expansion and operational deformation during prolonged use often compromise this symmetry, leading to gas flow inconsistencies. Consequently, the nozzle-type configuration has become the predominant choice in industrial planar cathode systems due to its mechanical robustness and operational reliability.

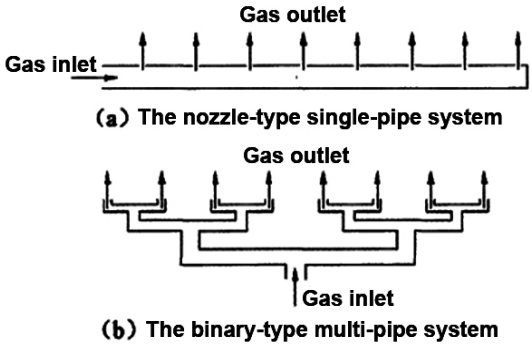


Fig. 2. Schematic diagrams of two gas distribution configurations

Despite its widespread adoption, the nozzle-type configuration has not been thoroughly investigated in practical production settings. Many manufacturers typically employ a simplistic approach by machining uniformly sized orifices along the distribution pipe, attempting to enhance gas uniformity by reducing orifice diameter or increasing pipe diameter. However, production data from industrial applications reveal that a significant proportion of coatings produced using this method still fail to meet uniformity specifications. This underscores the critical need for further optimization of gas distribution uniformity in cathode systems to achieve consistent coating quality.

After the gas is injected into the distribution pipe, it first flows out through the micro-orifices of the pipe and then diffuses spatially to the cathode target surface. The uniformity of gas distribution on the cathode target surface is primarily determined by two factors: (1) equal gas flow rates through each gas injection unit along the flow direction of the pipe, and (2) sufficient and uniform spatial diffusion of the discharged gas.

Ensuring equal gas flow rates through each gas injection unit is a prerequisite for achieving uniform gas distribution. If the orifice diameter and spacing remain unchanged, factors such as pressure drop along the pipe will inevitably lead to unequal gas flow rates through each orifice ($\Delta P \propto (L/D)\rho v^2$, $\Delta P$ is the gas pressure; $L$ is the length of gas flow path; $D$ is the total pipe length; $\rho$ denotes the density of the gas, and $v$ refers to its flow velocity) [13,14]. Therefore, the orifice spacing should gradually decrease along the gas flow direction, following a specific spacing variation pattern, to ensure equal gas discharge rates across all segments. Under the condition of equal gas discharge, achieving uniform gas distribution on the cathode target surface further requires ensuring the uniformity and sufficiency of gas diffusion from each orifice.

Therefore, this study focuses on the nozzle-type single-pipe configuration as the research object. First, the gas flow distribution in a pipe with gradually varying orifice spacing is simulated. Through analysis of the factors influencing gas distribution, structural modifications are proposed to optimize gas distribution.

## 3. Simulation Analysis

### 3.1. Gas Flow Simulation Modeling

The finite element method was employed to simulate the gas distribution in a single-pipe gas distribution system [15,16]. By comparing the gas distribution under conditions of equal and gradually varying orifice spacing, optimized results were obtained.

The simulation was performed using COMSOL Multiphysics software, specifically utilizing its three-dimensional laminar flow module. A 1:1 geometric model was constructed based on the dimensions of the gas distribution pipe. To compensate for pressure attenuation along the distribution line, the inter-hole spacing should follow a gradually decreasing arithmetic sequence. The spacing is calculated as:

$$d_n = d_1 - (n-1) \cdot \Delta d \ (n = 1,2,...,N) \tag{1}$$

Where: $d_1$ is initial hole spacing (recommended range: 60~75 mm), $\Delta d$ is decrement step length, $N$ is total number of gas holes. The optimal $\Delta d$ is determined through finite element simulation coupled with an iterative algorithm. The design target requires flow rate deviations ≤5% across all holes. During simulation, $\Delta d$ is systematically adjusted until achieving flow equilibrium conditions.

Fig. 3 shows the fluid domain model of the nozzle-type single-pipe system. To facilitate observation of the gas flow field distribution, in addition to establishing the fluid domain inside the gas distribution pipe, an extended fluid observation domain was created at the nozzle outlet, which is longer than the gas distribution pipe itself. This setup was used to examine whether the gas flow rates were equal across different sections.

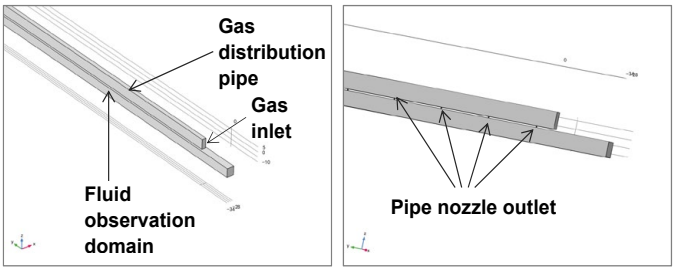


Fig. 3. Schematic diagram of the fluid domain model for the single-pipe gas distribution system

The computational domain and boundary conditions were configured as follows: The fluid domain was modeled as isothermal with a temperature of 25°C, and the flow model was set to laminar. The inlet boundary was defined as a velocity inlet, with a velocity of 0.04 m/s normal to the pipe entrance at the gas inlet end. The outlet boundary was set as a pressure outlet, with a static pressure of 0.5 Pa at the lower surface of the observation domain. All other surfaces were treated as no-slip, adiabatic walls.

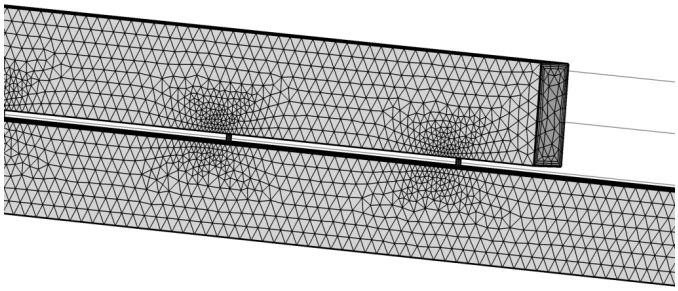

Fig. 4. Mesh refinement process

The fluid domain model was discretized using a global tetrahedral element division method, with the mesh correlation center set to "Coarse" for the initial division. Subsequently, local mesh refinement was implemented within the gas distribution hole regions, with a minimum element size of 0.1 mm. Special attention was given to achieving smooth transitional gradients between the refined zones and surrounding coarse-mesh areas, as illustrated in Fig. 4. The final computational model comprised 486,968 elements and 93,007 nodes, ensuring sufficient resolution for precision-critical simulations.

### 3.2. Comparison of Simulation Results

The gas flow distribution was simulated for two configurations: one with constant orifice spacing and the other with gradually varying orifice spacing. The results are as follows.

Fig. 5 shows the gas velocity distribution at the outlets for the constant orifice spacing configuration. It can be observed that the average gas velocity gradually decreases along the longitudinal direction of the pipe, with higher velocities at the upstream outlets and lower velocities at the downstream outlets. As the gas travels along the pipe, both velocity and pressure continuously decrease, resulting in reduced flow rates at outlets with the same orifice size along the pipe. This phenomenon justifies the use of varying orifice spacing to regulate flow rates and

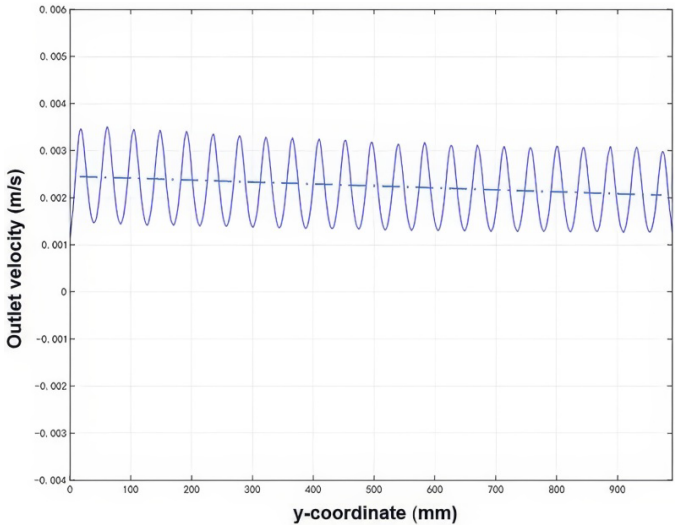


Fig. 5. Outlet velocity distribution for constant orifice spacing

achieve equal gas discharge. Additionally, the flow direction at the outlets exhibits fluctuations, with higher flow rates directly opposite the orifices and lower flow rates between them. These non-uniformities will be addressed by enhancing gas collision and mixing to achieve velocity uniformity.

Fig. 6 shows the gas velocity distribution at the outlets for the gradually varying orifice spacing configuration. It is evident that the average gas velocity remains consistent across all outlets, and the flow field distribution exhibits excellent similarity and uniformity. This indicates that the uniformity of the flow field distribution at the outlets is significantly improved after adjusting the orifice spacing.

In summary, for the nozzle-type single-pipe gas distribution system, the method of varying orifice spacing ensures nearly identical gas flow rates through all orifices. Compared to the constant orifice spacing configuration, the gas discharge uniformity is significantly improved, validating the earlier hypothesis.

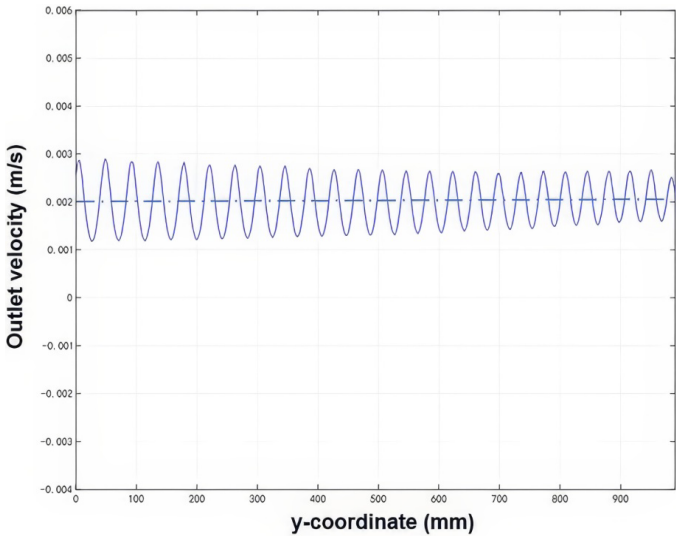


Fig. 6. Outlet velocity distribution for gradually varying orifice spacing

### 3.3. Optimization and Analysis of Gas Distribution Structure

Due to the orifice jet effect and the limited distance between the gas distribution pipe and the cathode target surface, the discharged gas often fails to fully diffuse before reaching the target surface. This results in significant differences in gas flow distribution between regions directly opposite the orifices and those between them. To achieve the ultimate goal of uniform gas distribution on the cathode target surface, further optimization of the gas distribution structure is necessary, in addition to adjusting the orifice spacing.

Fig. 7 shows a schematic diagram of the optimized gas distribution structure for the cathode target. To mitigate the jet effect at the orifices, the gas distribution pipe's orifices are oriented downward, increasing the diffusion space before the gas reaches the target surface. This design enhances the probability of molecular collisions (both intermolecular and molecule-wall interactions), thereby promoting more uniform gas mixing. The effectiveness of this optimized structure in improving gas distribution uniformity is validated through finite element modeling and gas flow simulation.

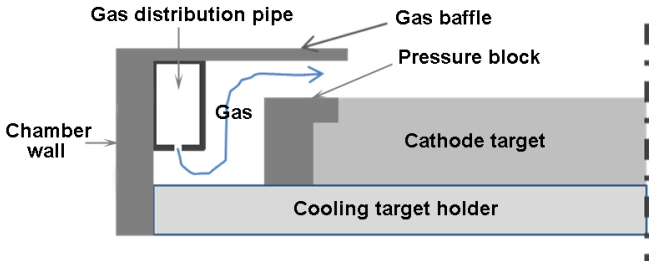


Fig. 7. Schematic diagram of the optimized gas distribution structure

A 1:1 simulation model of the cathode target surface was established. To reduce computational load, a symmetric model was used to calculate the flow field distribution on the cathode target, as shown in Fig. 8.

The model was discretized with mesh refinement applied to the regions around the gas distribution orifices. The mesh division is illustrated in Fig. 9. The final model consisted of 1,355,970 elements and 463,527 vertices.

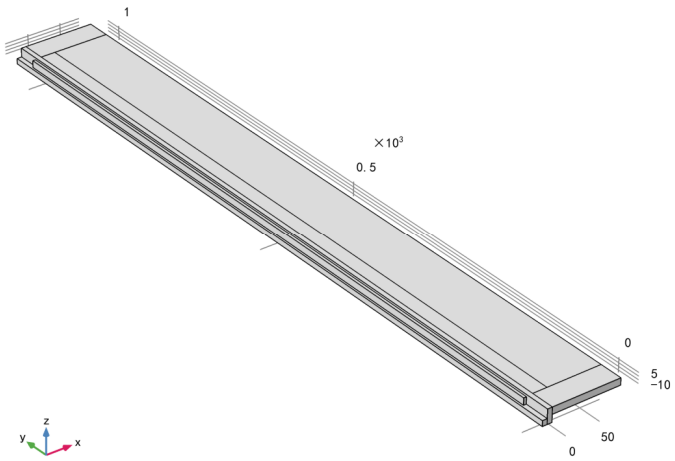


Fig. 8. Modeling of the cathode target structure

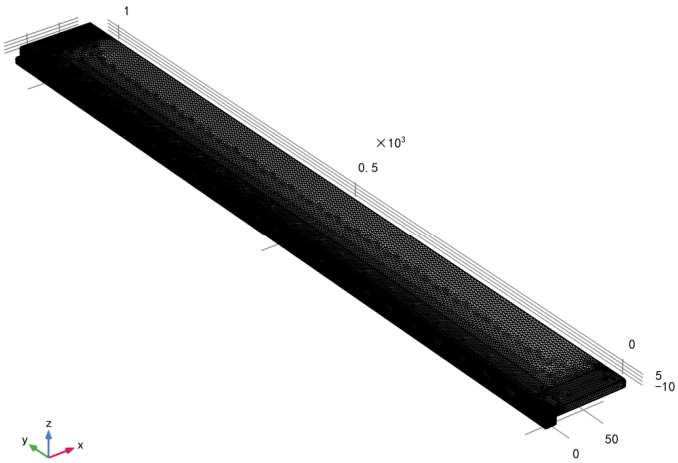


Fig. 9. Mesh division of the model

The simulation results provide the optimized gas flow field distribution, as shown in Fig. 10. After exiting the orifices, the gas diffuses and flows toward the target surface. For quantitative analysis, the gas velocity distribution at the target edge is shown in Fig. 11. Under different flow velocities, the gas velocity on the target surface achieves excellent consistency. As the gas exits the orifices, undergoes diffusion and reflection, the orifice jet effect is gradually weakened, resulting in highly uniform gas velocity across the entire target surface.

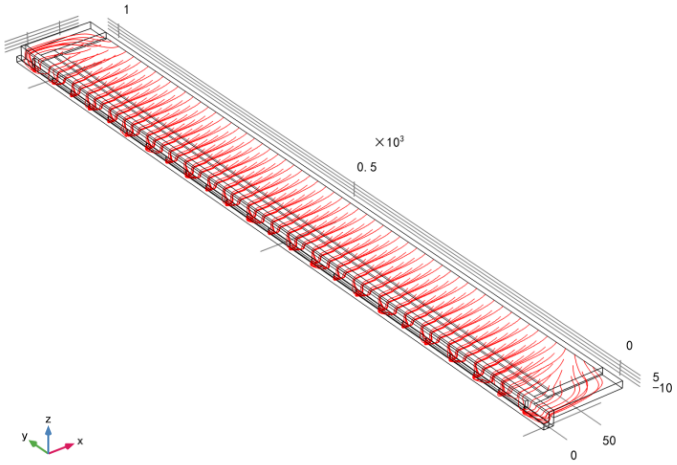


Fig. 10. Gas flow field distribution on the cathode target

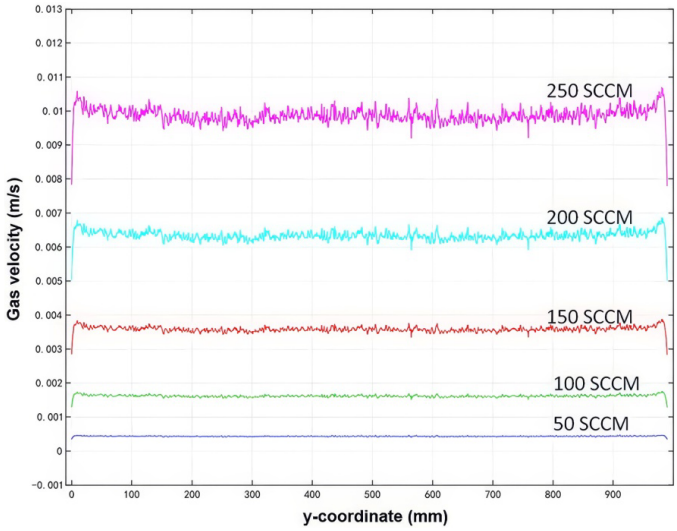


Fig. 11. Gas velocity distribution at the target edge

## 4. Experimental Verification

### 4.1. Experimental Conditions

To compare the effects of different gas distribution structures on tool color variation, experiments were conducted using a self-developed LIP1400 multi-arc ion plating system. The vacuum chamber had an effective deposition area of Φ900 mm × H1000 mm. The gas distribution pipe was 1.2 m long with 24 orifices, each 0.5 mm in diameter. Two gas distribution configurations were tested: (1) uniform orifice spacing and (2) gradually decreasing orifice spacing following an arithmetic sequence. Two sets of M2 high-speed steel tool samples, totaling six pieces, were used. Each set included three samples positioned uniformly at the top, middle, and bottom of the chamber height. Prior to coating deposition, the vacuum chamber was maintained at 200°C with a base pressure of $5\times10^{-3}$ Pa. Substrate surfaces were subjected to 30 minutes Ar glow discharge etching under a negative bias voltage of 600 V. Subsequently, TiCN coatings were deposited using identical process parameters, with key deposition conditions summarized in TABLE 1.

TABLE 1

Key TiCN coating process parameters

| Process Parameter | Arc Current (A) | Bias Voltage (V) | $N_2$ (sccm) | $C_2H_2$ (sccm) | Ar (sccm) | Deposition Time (min) |
|---|---|---|---|---|---|---|
| Value | 70 | 120 | 410 | 35 | 250 | 60 |

Coating composition was analyzed using a JSM-6701F cold field emission scanning electron microscope equipped with energy-dispersive X-ray spectroscopy (EDS). The analysis was performed at an acceleration voltage of 20 kV, magnification of 25×~650,000×, beam current of $1\times10^{-13}$ A~$2\times10^{-9}$ A, and a working distance of 6.5 mm.

### 4.2. Experimental results and discussion

Fig. 12 displays the characteristic EDS spectrum of the TiCN-coated cutting tool specimen. The analysis clearly identifies titanium (Ti), carbon (C), and nitrogen (N) as the primary coating constituents, with Ti showing the dominant spectral peak. Peaks associated with the M2 high-speed steel substrate composition have been excluded from presentation to maintain focus on the coating elements.

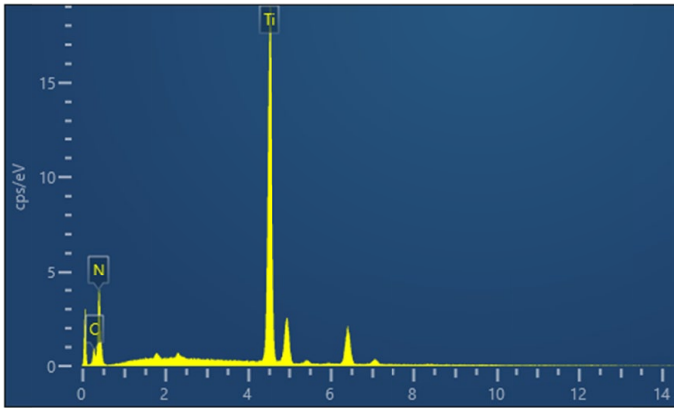


Fig. 12. EDS spectrum of the TiCN-coated tool specimen

TABLE 2 presents the composition analysis results for samples under different gas distribution structures. Under uniform orifice spacing, carbon (C) content exhibited significant

TABLE 2

EDS Analysis results of TiCN coating composition for different gas distribution structures

| Gas Distribution Structure | Sample Position | Atomic Percentage (at.%) | | |
|---|---|---|---|---|
| | | Ti | N | C |
| Uniform Orifice Spacing | Top | 44.62 | 40.07 | 15.31 |
| | Middle | 50.12 | 38.42 | 11.46 |
| | Bottom | 55.03 | 36.79 | 8.18 |
| Gradually Decreasing Orifice Spacing | Top | 45.86 | 42.98 | 11.16 |
| | Middle | 47.21 | 41.32 | 11.48 |
| | Bottom | 46.81 | 41.93 | 11.26 |

axial gradients (top-to-bottom), whereas nitrogen (N) variations remained marginal. This is attributed to the much lower flow rate of acetylene ($C_2H_2$) compared to nitrogen ($N_2$), leading to pronounced velocity and pressure attenuation along the gas flow path. The significant variation in C content caused noticeable color differences, as shown in Fig. 13a. The top sample exhibited a dark yellowish-brown hue, the middle sample a rose-gold color, and the bottom sample a light yellow tone. This inhomogeneity stems from pronounced velocity/flow rate gradients across positions, disrupting plasma stability and TiCN synthesis uniformity on the tool surface.

In contrast, for the gradually decreasing orifice spacing configuration, the C content remained consistent across all positions, with a deviation of less than 10%. As shown in Fig. 13b, the samples displayed a uniform rose-gold color. This uniformity is achieved because the gas flow velocity and rate are consistent across all orifices, with minimal gradient differences. Additionally, the downward-oriented orifices allow the gas to first impact the chamber sidewalls, acting as a pressure buffer and promoting uniform gas distribution. This results in more uniform plasma density at the cathode target, leading to consistent TiCN coating coloration across the top, middle, and bottom samples.

## 4. Conclusion

(1) This study addresses the challenge of coating appearance uniformity in industrial-scale PVD coating production by analyzing the factors influencing uniform gas distribution. Focusing on a single-pipe nozzle-type gas distribution system, the effects of different orifice arrangements on gas flow field distribution were investigated. Finite element simulations were used to compare the flow field characteristics of uniform and gradually decreasing orifice spacing configurations. Further structural optimization eliminated the orifice jet effect, achieving uniform gas distribution at the target surface.

(2) Experimental validation confirmed the effectiveness of the optimized structure. Tools coated using the gradually decreasing orifice spacing configuration exhibited significantly improved appearance uniformity. EDS analysis revealed that the C content deviation across the top, middle, and samples was less than 10%. This innovative solution requires only straightforward modifications to the gas distribution piping system, eliminating the need for complex symmetrical structures or high-precision assembly. Particularly suitable for retrofitting existing PVD coating equipment, the proposed approach effectively resolves the persistent challenge of axial deposition non-uniformity, thereby significantly enhancing both coating product appearance and quality.

**Founding**

Lanzhou Talent Entrepreneurship and Innovation Project(2022-RC-3).

## REFERENCE

[1] A. Baptista, F. Silva Jacobo Porteiro, et al., Sputtering Physical Vapor Deposition (PVD) Coatings: A Critical Review on Process Improvement and Market Trend Demands. Coatings **8** (11), 402 (2018). DOI: https://doi.org/10.3390/coatings8110402

[2] A. Baptista, F.J.G. Silva, J. Porteiro, et al., On the Physical Vapor Deposition (PVD): Evolution of Magnetron Sputtering Processes for Industrial Applications. Procedia Manufacturing **17**, 746-757 (2018). DOI: https://doi.org/10.1016/j.promfg.2018.10.125

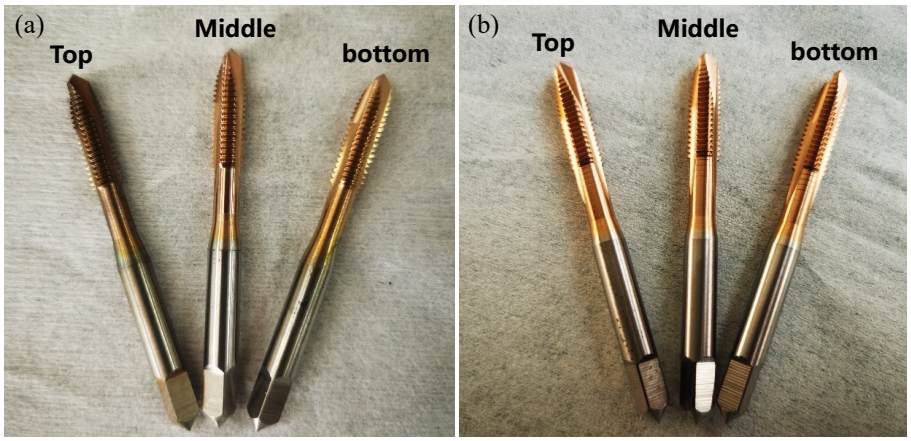


Fig. 13. TiCN-coated tool samples with different gas distribution structures, (a) Uniform Orifice Spacing, (b) Gradually Decreasing Orifice Spacing

[3] H. Ichou, N. Arrousse, E. Berdimurodov, et al., Exploring the Advancements in Physical Vapor Deposition Coating: A Review. Journal Bio-and Tribo-Corros. **10**, 3 (2024).
DOI: https://doi.org/10.1007/s40735-023-00806-0

[4] Rolf Hohl, PVD hard coating as a surface treatment in mass production requires new process technology for use on equipment and cleaning substrates. Metal Finishing **104** (6), 21-23 (2006).
DOI: https://doi.org/10.1016/S0026-0576(06)80242-4

[5] R.L. Boxman, P.J. Martin, D.M. Sanders, Handbook of Vacuum Arc Science and Technology. Park Ridge, New Jersey, U.S.A., Noyes Publications 1995, 367-396.

[6] Yongshuan Wu, Kefan Liu, Pengcheng She, et al., Simulation and optimization of reactor airflow and magnetic field for enhanced thin film uniformity in physical vapor deposition. Microelectronic Engineering **296**, 112294 (2025).
DOI: https://doi.org/10.1016/j.mee.2024.112294

[7] Zhijun Su, Xiaohua Jie, Wenfang Li, et al., Effect of C2H2 flow rate and a Ti/TiN/TiCN interlayer on the structure, mechanical and tribological properties of a-C:H films deposited using a hybrid PVD/PECVD process with an anode-layer ion source. Vacuum **209**, 111753 (2023).
DOI: https://doi.org/10.1016/j.vacuum.2022.111753

[8] Xin Ren, Ruishan Zhao, We Wang, et al., Corrosion Resistance of TiCN Films Prepared with Combining Multi-arc Ion Plating and Magnetron Sputtering Technique. Rare Metal Materials and Engineering **47** (7), 2028-2036 (2018).
DOI: https://doi.org/10.1016/S1875-5372(18)30176-0

[9] Totka Bakalova, Lucie Svobodová, Nikolay Petkov, et al., The effect of the process gas mixture ratio on the structure and composition of TiC and TiCN thin layers prepared by cathodic arc deposition on tool steel. Journal of Manufacturing Processes **93**, 90-100 (2023).
DOI: https://doi.org/10.1016/j.jmapro.2023.02.067

[10] Zhifeng Zeng, Yi Ruan, Zebing Xie, The Influence of the Working Gas in the Vacuum Sputtering Coater on the Chromatic Aberration of the Plating Articles. Mechanical & Electrical Engineering Technology **50** (04), 151-152+165 (2021).
DOI: https://doi.org/10.3969, j. issn. 1009-9492. 2021.04.039

[11] Carles Corbella, Upscaling plasma deposition: The influence of technological parameters. Surface and Coatings Technology **242**, 237-245 (2013).
DOI: https://doi.org/10.1016/j.surfcoat.2013.12.002

[12] Pengli Jin, Dezhi Xiao, Xiubo Tian, et al., Synergistically tailoring the distribution of precursor gas for uniform internal DLC coating of long tube. Surface and Coatings Technology **466**, 129661 (2023).
DOI: https://doi.org/10.1016/j.surfcoat.2023.129661

[13] Yichen Zhang, Vacuum coating equipment. Beijing, Metallurgical Industry Press 82-89 (2013).

[14] Shaojiang Huang, Hongxi Xie, Huijun Hou, et al., Design of gas distributor on plasma chemical vapor deposition. Journal of Guangdong Non-ferrous Metals **12** (1), 21-25 (2002).
DOI: https://doi.org/10.3969/j.issn.1673-9981.2002.01.006

[15] Kirsten Bobzin, Ralf Peter Brinkmann, Thomas Mussenbrock, et al., Continuum and kinetic simulations of the neutral gas flow in an industrial physical vapor deposition reactor. Surface and Coatings Technology **237** (25), 176-181 (2013).
DOI: https://doi.org/10.1016/j.surfcoat.2013.08.018

[16] S.N. Grigoriev, V.Yu. Fominski, A.G. Gnedovets, et al., Experimental and numerical study of the chemical composition of WSex thin films obtained by pulsed laser deposition in vacuum and in a buffer gas atmosphere. Applied Surface Science **258** (18), 7000-7007 (2012).
DOI: https://doi.org/10.1016/j.apsusc.2012.03.153